Palladium Nanoparticles Synthesized by Pulsed Electrolysis in Room-Temperature Ionic Liquid

Gwangwon Park[1], Jesik Park[1], YoungjuCho[2], Churl KyoungLee[1,]*

[1] School of Material Science & Engineering, Kumoh National Institute of Technology, Gumi, Gyungsangbuk-do 730-701, Republic of Korea
[2] R&D Center for Valuable Recycling, Daejeon, Republic of Korea
[*]E-mail: cklee@kumoh.ac.kr

Synthesis of palladium nanoparticles by pulsed electrolysis was investigated in the room-temperature ionic liquid 1-butyl-3-methylimidazolium chloride ([C$_4$mim]Cl) using palladium chloride (PdCl$_2$) as the palladium source. A palladium-coated carbon (Pd/C) catalytic electrode was synthesized by direct deposition of palladium on a carbon paper working electrode. The size and distribution of the palladium particles were easily controlled by varying the electrolysis conditions such as the overpotential, holding time of the applying potential, and temperatures. The composition, crystal structure, and morphology of the palladium were confirmed by scanning electron microscopy combined with energy dispersive spectroscopy and transmission electron microscopy. The uniformly distributed palladium nanoparticles had an average size of 3.6 nm with a standard deviation of 0.4.

1. INTRODUCTION

Palladium is a precious metal belonging to the platinum group metals (PGMs) and has the lowest melting temperature of the PGMs. Nano-palladium is considered a prospective alternative for use in the catalytic electrode of fuel cells based on its ability to adsorb and release hydrogen. Nano-palladium is also used as a catalyst to purify automobile exhaust gas, as well as in many other processes such as chemical processes, photovoltaic materials, electrical materials, sensors, prosthetic materials, surgery, jewelry, etc [1-8]. Platinum has remained the most commonly used catalytic material since William Grove and co-workers first developed the fuel cell by employing electrolysis in diluted sulfuric acid using a platinum electrode to generate an electrical current [9]. The electrode of the early fuel cell was loaded with about 25 mg/cm^2 of platinum. However, more recently, the amount

of platinum used in the fuel cell has been reduced to less than 0.45 mg/cm^{2}as a means of circumventing the high price of platinum as well as due to modification of the catalytic electrode [10].

Nevertheless, platinum has attendant issues such as electrolyte poisoning by carbon monoxide and degradation by platinum corrosion. However, the major drawback of the commercial fuel cell is the highly prohibitive price of the platinum catalyst. Platinum is the most costly PGM and is about 10 times more expensive than palladium, rhodium, and ruthenium. Therefore, the research focus has recently shifted to finding alternatives to platinum [11]. The chemical combination of the platinum and other metals or organic materials and the structural changes of the catalyst materials have been studied. For example, transition metals such as iron, cobalt, nickel and their alloys have been investigated as catalytic materials for the fuel cell and other chemical processes. Many other studies to coordinate catalytic materials based on iron and cobalt bonded to organic polymers have also been undertaken [12-15]. Furthermore, single metal or alloy complexes of PGMs such as palladium, iridium, rhodium, ruthenium, and osmium are being developed as alternatives to platinum [16]. As a catalytic material for the oxygen reduction reaction, palladium has the next highest reactivity as a single metal after platinum. For this reason, palladium is a prime candidate as a single metal to replace platinum [17].

The synthesis of nano-catalysts is an extensive and complex process with long reaction times and difficulties in controlling the particle size. These synthetic methods include electroless deposition, the polyol method, sputtering, the γ-irradiation method, the micro-emulsion method, aerosol-assisted deposition (AAD), the Pechini method, supercritical deposition, the hydrothermal method, and the colloid method [18]. However, these methods have many shortcomings such as complex and time-consuming processes and the use of toxic additives and extreme environments such as vacuum or high pressure and temperature. In contrast, electrolysis is a simple process that can yield an accurately controllable composition, particle size, and distribution of the catalyst by variation of the current or potential. This method may also be advantageous for continuous and mass production.

Ionic liquids are eco-friendly and comprised only of cations and anions. They have low vapor pressure and are electrochemically stable. By varying the combination of cations and anions, ionic liquids with favorable properties can be judiciously designed. Therefore, the application of ionic liquids is actively being studied in various segments of electrochemistry. The redox behavior of ionic liquids during electrolysis differs from that of aqueous solutions. Therefore, ionic liquids can be effectively used to obtain highly active metals that are difficult to reduce in aqueous electrolytes. Moreover, electrolytes based on ionic liquids are thermally and chemically stable, which minimizes their adverse environmental effects due to the stability of ionic liquids over long periods of operation [19].

In this study, the electrochemical behavior of palladium in the ionic liquid [C$_4$mim]Cl was studied via pulsed electrolysis. A catalytic palladium electrode with well-distributed nano-sized particles was also synthesized and the effect of the electrolysis conditions on the reduction behavior, crystal size, and size distribution of palladium was also evaluated. The conditions varied include the electrolyte composition, temperature, potential or current, duty factor, and duration of electrolysis. The morphology, particle size, and crystallinity of palladium were analyzed by field emission scanning electron microscopy and transmission electron microscopy. The purity of the palladium nanoparticles was assessed by energy-dispersive spectroscopy.

2. EXPERIMENTAL

A three-electrode system was employed to study the electrochemical behavior of palladium in [C$_4$mim]Cl (Aldrich, ≥98.0%). A carbon paper (JNTG, JNT-20) was used as a working electrode and platinum wire was used as a counter and reference electrode (platinum quasi-reference electrode, Pt-QRE).Although most palladium salts can be used to synthesize palladium nanoparticles, PdCl$_2$ (Kojima Chemicals Co., Ltd., ≥99%) was selected because of its favorable solubility, conductivity, and redox behavior in the ionic liquid, [C$_4$mim]Cl [20]. All ionic liquids used herein were dried at 100 ℃ for 24 h to remove trace amounts of water, and all electrodes and cells were cleaned prior to the experiments by using a 1:1 (v/v) mixture of sulfuric acid (H$_2$SO$_4$) and hydrogen peroxide (H$_2$O$_2$) solutions.

The potential stability ranges and the effect of the electrolysis conditions on the electrochemical properties of the ionic liquids were measured by cyclic voltammetry using a Potentiostat/Galvanostat (Electrochemical Interface SP-240, Bio-logic Analytical) at a scan rate of 10 mV/s in the potential range between -2 V and 0.5 V (vs. Pt-QRE). The effects of the electrolysis conditions (temperature: 90 to 150 ℃, overpotential: -1 to -3.8 V, duty factor: 0.2 to 0.5, and pulse duration: 2 to 10 s) on the redox reaction and size distribution of the palladium deposits were evaluated. Direct reduction of PdCl$_2$ dissolved in the [C$_4$mim]Cl was conducted to reduce metallic palladium for direct synthesis of the nanoparticles on the metal or carbon electrodes.

In order to analyze the morphology, particle size, and crystallinity of the palladium particles, a field emission scanning electron microscope (FE-SEM, JEOL, JSM6701F) with an energy dispersive spectrometer (EDS) and a transmission electron microscope (TEM, JEOL, JEM-2100, JEM-ARM200F) were used. The porosity of the carbon paper (used as the working electrode) was measured with a BET & Pore Size Analyzer (BELSORP-max).

3. RESULTS AND DISCUSSION

3.1 Electrochemical behavior of palladium

Considering the solubility and electrochemical behavior of PdCl$_2$, the ionic liquid [C$_4$mim]Cl was used as the solvent. Carbon paper was used as the working electrode and platinum wire was used as the counter and reference electrodes. The calculated specific surface area of carbon paper determined by the BET method using nitrogen gas at 77 K was 0.775 m^2/g. Fig. 1 shows cyclic voltammograms of [C$_4$mim]Cl with and without palladium, acquired at 130 ℃ at a scan rate of 10 mV/s in the potential range of -2 to 0.5 V (vs. Pt-QRE).

[C$_4$mim]Cl was stable over 1.5 V (or over the range of -1.7 ~ 0.2 V, vs. Pt-QRE). The potential stability range did not change with the introduction of palladium ions. The electrolyte was suitable for the electrolysis of palladium because the redox reaction of palladium occurs within the potential stability range of the electrolyte.
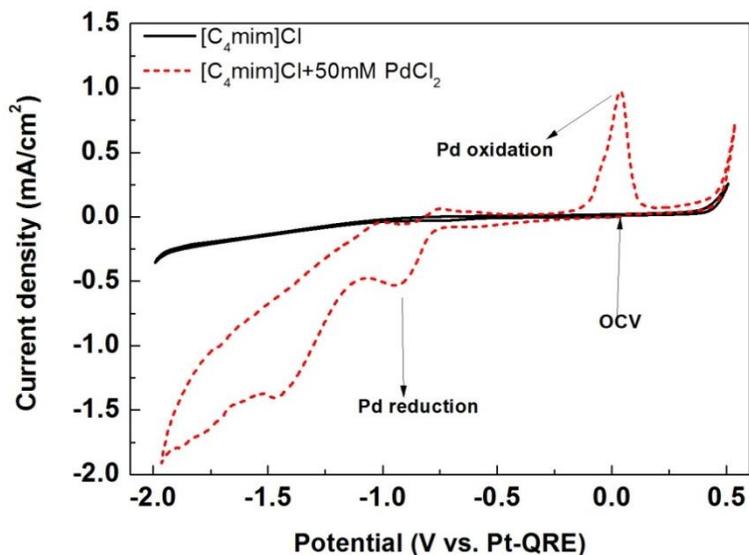
Figure 1. Cyclic voltammetry of [C$_4$mim]Cl with/without palladium on carbon

The reduction potentials were -0.92 V and -1.4 V (vs. Pt-QRE) and the corresponding oxidation potential was 0.15 V. The oxidation (dissolution) of palladium in [C$_4$mim]Cl may be achieved in a one-step reaction; on the other hand, the reduction is a two-step process. It could be assumed that nucleation and crystal growth of palladium occurred sequentially at different potentials and the redox reaction of palladium in [C$_4$mim]Cl exhibited a symmetric behavior.

When the electrolysis was conducted at -1 V (vs. Pt-QRE) for 30 min on carbon electrode, metallic palladium could be obtained and no impurities were detected on EDS shown in Fig. 2. It means that electrolysis of palladium in non-aqueous electrolyte such as [C$_4$mim]Cl can apply on synthesis of catalytic electrode loaded palladium.
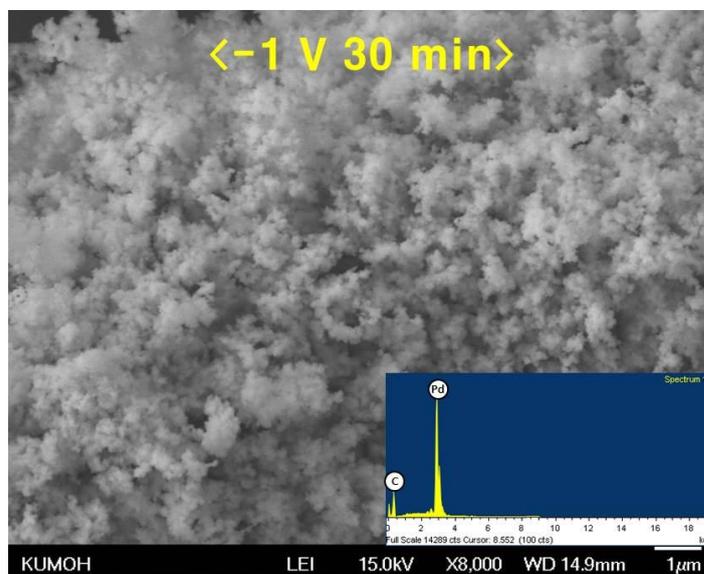
Figure 2. Morphology of palladium electrodeposited at -1 V (vs. Pt-QRE) on carbon electrode

3.2 Pulsed electrolysis in [C$_4$mim]Cl electrolyte

Facile control of the particle size and distribution of the reduced deposits of palladium can be achieved by reduction of palladium at an extremely high potential or current. Furthermore, by using ionic liquids that do not contain hydrogen and water, hydrogen pollution could be avoided. Furthermore, due to their low vapor pressure and chemically and electrochemically outstanding stability, ionic liquids can withstand processing for long durations in the presence of the dissolved palladium salts; this causes almost no waste to be generated during processing [19].

Fig. 3 shows the pulse waveform for synthesis of the palladium nanoparticles. The waveform is a combination of the peak time while applying a specific potential or current and the rest time from open circuit voltage (OCV, equilibrium potential). The high peak potential or current might be favorable for promoting nucleation rather than crystal growth; in addition, no contamination by non-metallic impurities such as hydrogen and oxygen was detected. The rest time at the OCV can be recovered concentration of palladium on the electrode surface.
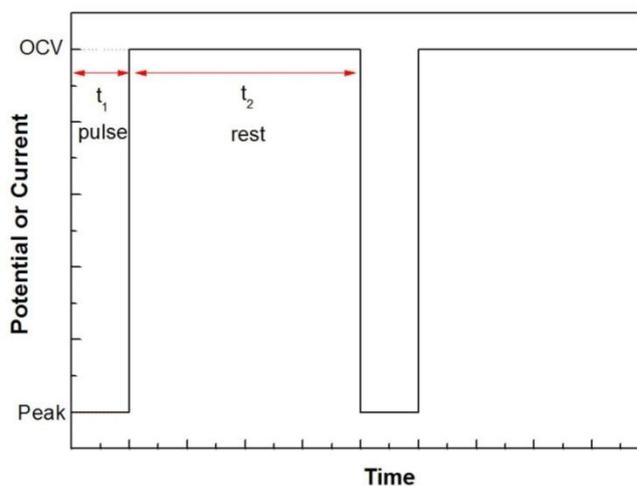
Figure 3. Pulse waveform for synthesis of palladium nanoparticles.

As it is shown in the following equation, duty factor is the ratio occupied by on time (t$_1$) in a cycle (t$_1$ + t$_2$).

$$\text{Duty factor} = \frac{t_1}{t_1 + t_2}$$

3.2.1. Effect of duty factor

Palladium particles were synthesized at 110 ℃ and 130 ℃ using a palladium concentration of 0.05 M, reduction potential of -0.85 V, pulse time (t$_1$) of 10 ms, and pulse duration of 2 s. The palladium nanoparticles were uniformly distributed on the carbon paper, as shown in the SEM image

presented in Fig. 4. The average particle size was calculated as the arithmetic mean and standard deviation using at least 50 particles.
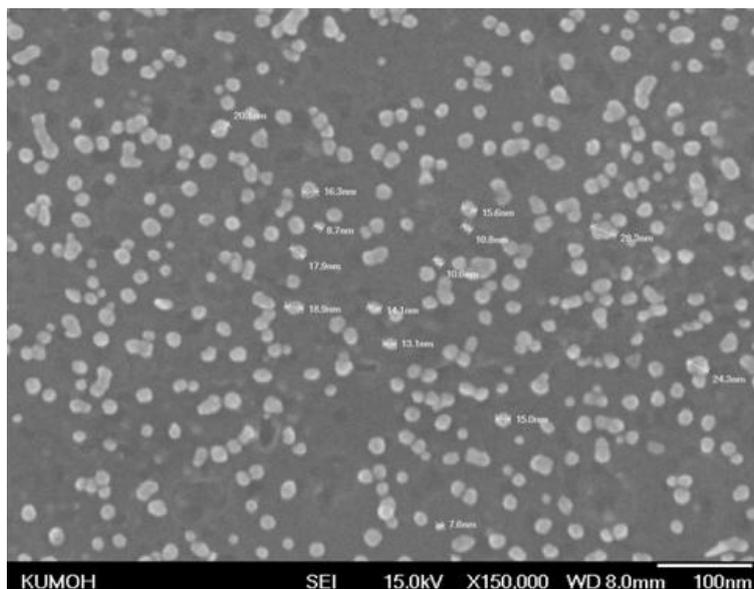
Figure 4. SEM image of palladium nanoparticles synthesized by pulse electrolysis (130 ℃, $PdCl_2$ 0.05 M, -1.85 V, 10 ms t_1, 0.5 duty factor, 2 s pulse duration).
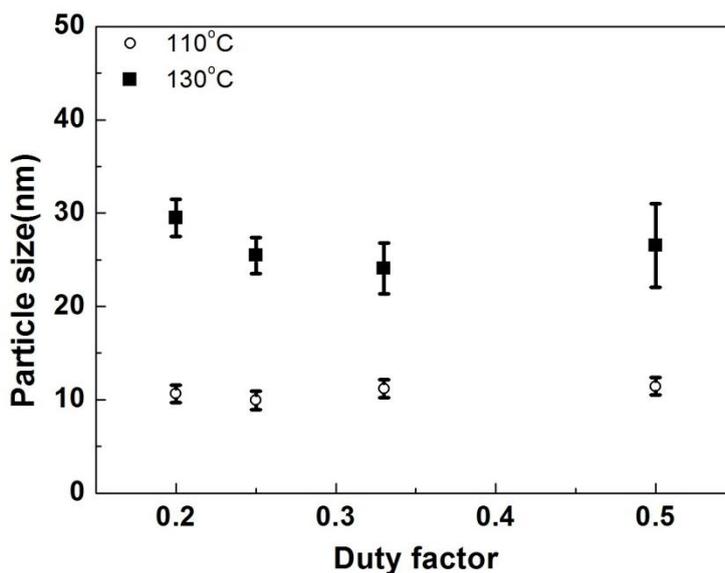
Figure 5. Effect of duty factor on the particle size of palladium ($PdCl_2$ 0.05 M, -1.85 V, 2 s pulse duration).

The effect of the duty factor on the particle size is presented in Fig. 5. The figure shows that palladium nanoparticles with an average size between 11 nm and 27 nm could be easily synthesized in a very short time by pulsed electrolysis. At 130 ℃, the average size of the particles was 26.4 nm and

the standard deviation was 2.8. In comparison, the average size of the particles prepared at 130 ℃ was 10.8 nm and the standard deviation was 0.9. The significant changes were predicted by controlling duty factor because concentrations of palladium ions around the electrode are changed with changing pulse time (t_1). But there was a slight variation of the particle size with changes in the duty factor although the change of temperature caused the significant change of the particle size.

3.2.2. Effect of overpotential

Fig. 6 shows the effect of the overpotential on the particle size at a palladium concentration of 0.05 M, using temperatures of 110 ℃ and 130 ℃, a pulse time (t_1) of 10 ms, a duty factor of 0.5, and pulse duration of 2 s. The particle size decreased significantly as the overpotential increased. This means that an increase in the overpotential led to an increase in the rate of palladium reduction on the electrode surface. Nucleation of palladium might be dominant compared to crystal growth due to the extremely high potential; thus, the palladium particles became smaller and uniform. In other words, the synthesis of nanoparticles having an average size of 6 ~ 19 nm with narrow size distributions could be simply achieved by changing the electrolysis conditions such as the applied potential. The reaction was also completed in only a few seconds.
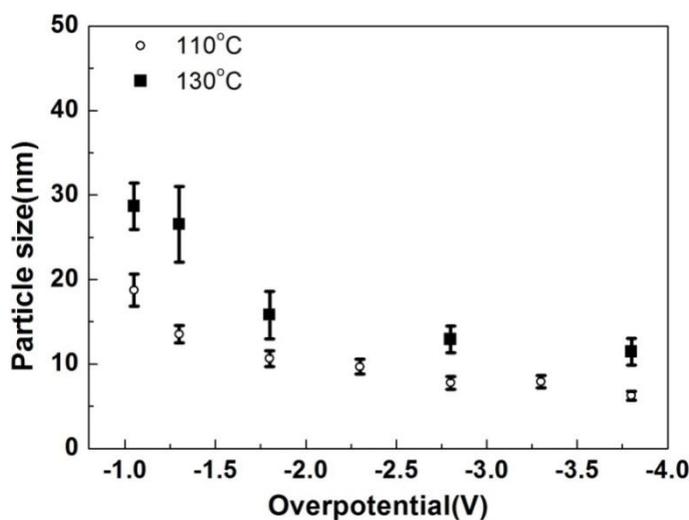
Figure 6. Effect of overpotential on the particle size of palladium ($PdCl_2$ 0.05 M, t_1 10 ms, duty factor 0.5, pulse duration 2 s).

3.2.3. Effect of pulse duration and temperature

Fig. 7 shows the effect of the pulse duration on the particle size at a concentration of 0.05 M, temperatures of 110 ℃ and 130 ℃, pulse time (t_1) of 10 ms, and duty factor of 0.5. With increasing pulse duration, the particle size increased to a certain point. Increasing the pulse duration caused an increase of the particle size due to preferential crystal growth.
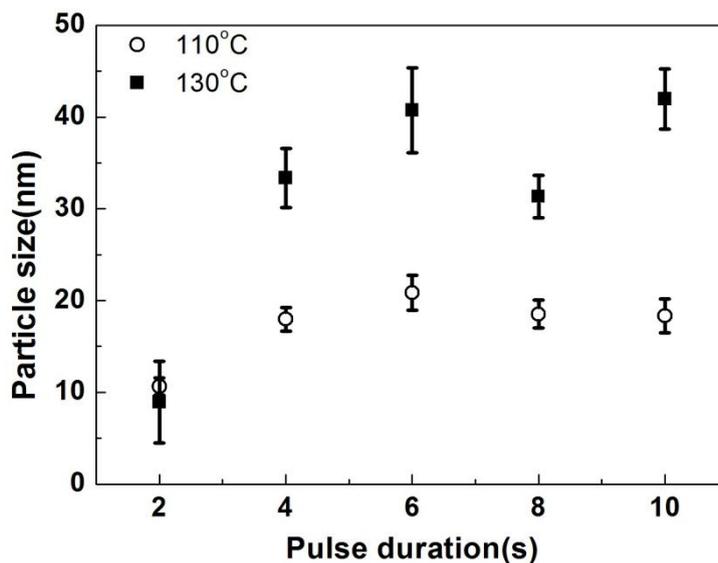
Figure 7. Effect of pulse duration on the particle size of palladium (PdCl$_2$ 0.05 M, -1.85 V, t$_1$ 10 ms, duty factor 0.5).
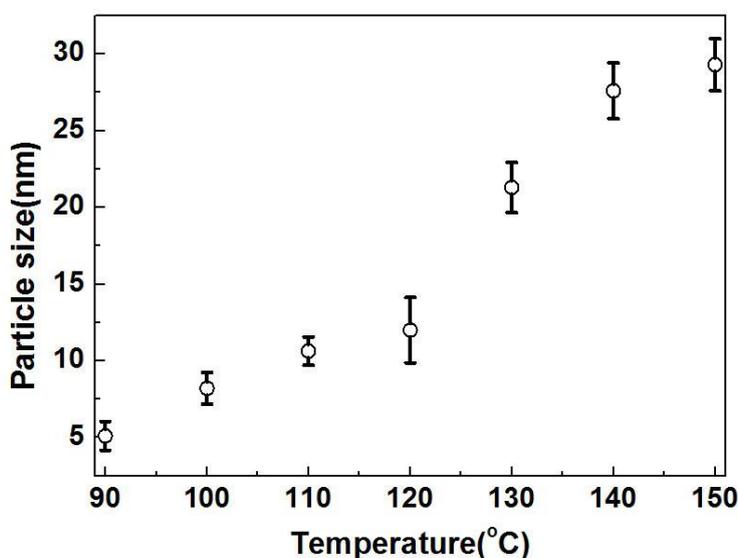
Figure 8. Effect of temperature on the particle size of palladium (PdCl$_2$ 0.05 M, -1.85 V, t$_1$ 0 ms, duty factor 0.5, pulse duration 2 s).

The effect of temperature on the particle size is shown in Fig. 8 when the palladium concentration was 0.05 M, using a pulse time (t$_1$) of 10 ms, duty factor of 0.5, and pulse duration of 2 s. With increasing temperature, the particle size also increased given that increasing the temperature increases the rate of diffusion of palladium on the electrode surface. Thus, the increased palladium concentration on the electrode surface led to dominant crystal growth of the palladium particle relative to nucleation. With increasing temperature, the particle size and standard deviation of the palladium particles increased.

3.3 Crystallinity analysis

The morphology of the palladium nanoparticles, identified by TEM, is presented in Fig. 9 for nanoparticles generated using a palladium concentration of 0.05 M, reduction potential of -1.85 V, temperature of 90 ℃, pulse time (t_1) of 10 ms, duty factor of 0.5, and pulse duration of 4 s. The average particle size was 3.6 nm and the standard deviation was 0.4as measured by TEM.

S. H. Joo et al. reported that the optimum size of catalytic materials is approximately 3.3 nm on the oxygen reduction and methanol oxidation reaction [21]. Furthermore, Kinoshita et al. reported that catalysts with dimensions of less than 2 nm suffer from disadvantages such as low catalytic characteristics in the oxygen reduction reaction because low coverage of hydroxyl (OH) groups in the oxygen reduction reaction cannot be obtained as the capacity of the particles to adsorb carbon monoxide (CO)and OH increases with decrease in the particle size; however, the large surface area is advantageous for oxygen reduction [22].
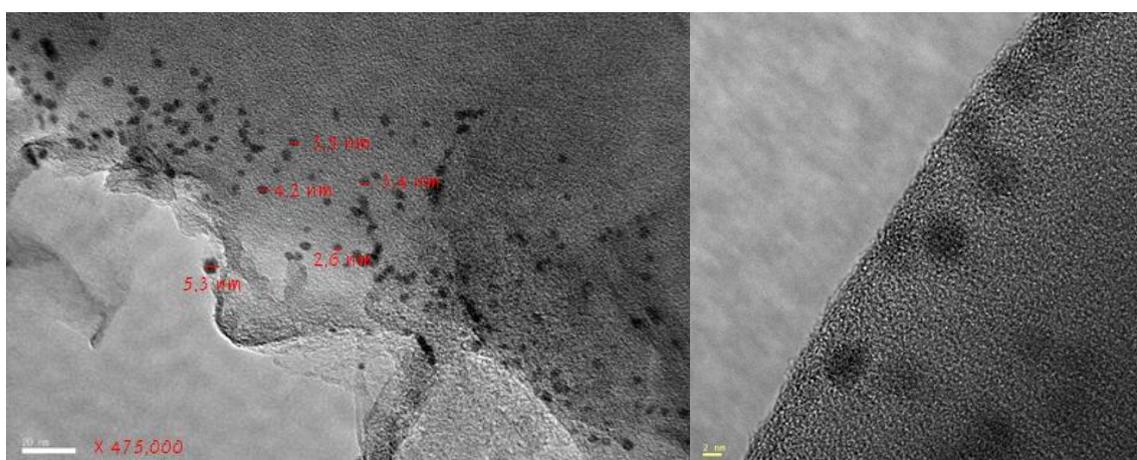
Figure 9. TEM images of the palladium nanoparticles (PdCl$_2$ 0.05 M, 90 ℃, -1.85 V, t_1 10 ms, duty factor 0.5, pulse duration 4 s).
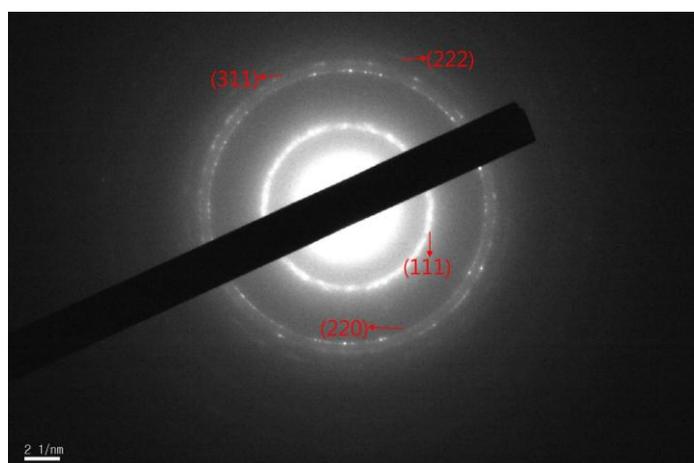
Figure 10. TEM diffraction pattern of the palladium nanoparticle (PdCl$_2$ 0.05 M, 90 ℃, -1.85 V, t_1 10 ms, duty factor 0.5, pulse duration 4 s).

Fig. 10 shows the TEM diffraction pattern of palladium synthesized by pulsed electrolysis. From the ring pattern, it could be determined that the particles of palladium have the face centered cubic structure (FCC), not amorphous, and uniformly distributed.

4. CONCLUSION

Synthesis of palladium nanoparticles with a narrow size distribution was achieved by simple non-aqueous electrolysis requiring only a few seconds with no contamination by non-metallic impurities such as hydrogen. The use of an extremely high potential and a rest time during pulsed electrolysis promoted nucleation during the palladium reduction in preference to crystal growth. Non-aqueous electrolytes such as the ionic liquid [C$_4$mim]Cl could influence the diffusion rate of the palladium ions over a wide range compared with aqueous media. The effect of the duty factor of the pulse wave was insignificant, whereas decreasing the applied potential and increasing the pulse duration and temperature increased the average size of the palladium particles. The uniformly distributed palladium nanoparticles had an average size of 3.6 nm with a standard deviation of 0.4.

References

1. T. Kendall, *Platinum Met. Rev.*, 48 (2004) 13
2. J. Tsuji, *Palladium reagents and catalysts: New perspectives for the 21st century,* 2nd ed., John Wiley and Sons, Japan (2004)
3. J. Shu, B. P. A. Grandjean, A. Vanneste, S. Kaliaguine, *Can. J. Chem. Eng.*, 69 (1991)1036
4. T. H.Allen, W. S.Root, *J. Biol. Chem.*, 216 (1955) 319
5. F. D. Manchester, A. San-Martin, J. M. Pitre, *J. Phase Equilib.,* 15 (1994) 62
6. N.N. Greenwood, A. Earnshaw, *Chemistry of the Elements*, 2nd ed., Butterworth–2 Heinemann, Oxford, U.K. (1997)
7. W. Grochala, P. P. Edwards, *Chem. Rev.*, 104 (2004) 1283
8. M. Ware, *Platinum Met. Rev.*, 49 (2005) 190
9. W. R. Grove, M. A. Esq, *Philos. Mag.*,14 (1839) 127
10. S. D. Lim, *SAREK*, 41 (2012) 26
11. K. J. Kwon, *J. Korean Electrochem. Soc.*, 15 (2012) 12
12. R. Bashyam, P. Zelenay, *Nature*, 443 (2006) 63
13. G. Wu, K. L. More, C.M. Johnston, P. Zelenay, *Science*, 332 (2011) 443
14. B. Wu, N. Zheng, *Nano Today*, 8 (2013) 168
15. F. Kettemann, M. Wuithschick, G. Caputo, R. Kraehnert, N. Pinna, K. Rademann, J. Polte, *Cryst. Eng. Comm.*, 17 (2015) 1865
16. V. R. Stamenkovic, B. S. Mun, M. Arenz, K. J. J. Mayrhofer, C. A. Lucas, G. Wang, P. N. Ross, N. M. Markovic, *Nature Mater.*, 6 (2007) 241
17. J. K. Norskov, J. Rossmeisl, A. Logadottir, L. Lindqvist, J. R. Kitchin, T. Bligaard, H. Jonsson, *J. Phys. Chem. B*, 108 (2004) 17886
18. A. Esmaeilifar, S. Rowshanzamir, M.H. Eikani, E. Ghazanfari, *Energy*, 35 (2010) 3941

19. C.A. Nieto de Castro, *J. Mol. Liq*., 156 (2010) 10
20. M. Jayakumar, K.A. Venkatesan, T.G. Srinivasan, *Electrochim. Acta*, 52 (2007) 7121
21. S. H.Joo, K. J. Kwon, D. J. You, C. H. Pak, H. Chang, J. M. Kim, *Electrochim. Acta*, 54 (2009) 5746
22. N. Giordano, E. Passalacqua, L. Pino, A. S. Arico, V. Antonucci, M. Vivaldi, K. Kinoshita, *Electrochim. Acta*, 36 (1991) 1979